Impact of Key Circuit Parameters on Signal-to-Noise Ratio Characteristics for the Radio Frequency Single-Electron Transistors

M. Manoharan, Benjamin Pruvost, Hiroshi Mizuta, *Member, IEEE*, and Shunri Oda, *Member, IEEE*

***Abstract*—Hybrid simulation was performed to analyze the response of the real-time reflection-type radio frequency single-electron transistor (RF-SET) measurement system. A compact and physically-based analytical SET model, which was validated with a Monte Carlo simulator, was used to simulate the SET characteristics, while SPICE equivalent circuits were implemented to simulate all other components of the RF-SET measurement system. The impact of various key parameters on the RF-SET response was demonstrated for a carrier frequency much less than *I*/*e* (*I* is the typical current through the SET). It was revealed that an inevitable feed-through loss between the tank circuit and the cryogenic amplifier, and high-frequency parasitics of the inductor degrade the RF-SET performance significantly. As such, they have to be optimized to experimentally realize the shot-noise-limited charge sensitivity.**

***Index Terms*—Analog hardware description language (AHDL), analytical model, charge sensitivity, hybrid simulation, radio frequency SET (RF-SET), single-electron transistor (SET).**

I. Introduction

THE HIGH charge sensitivity of the single-electron transistor (SET) can be used to measure the signal near quantum limitation [1]. However, the typical SET resistance of 100 kΩ and lead capacitance of 1 nF at the output restrict the measurement bandwidth to a few kilohertz or less, which leads to a low operating speed and a $1/f$ noise impairment. Rather than carrying out standard voltage and current measurements, the radio frequency SET (RF-SET) adopts the measurement of RF waves reflected [2] and transmitted [3] from and across the SET using an *LC*-resonant circuit (invariably used as "tank circuit" in this paper) for impedance matching. This novel concept helps to realize a high charge sensitivity of $0.9 \times 10^{-6}\ e/\sqrt{\text{Hz}}$ [4] and a measurement bandwidth of more than 100 MHz [2]. Due to these remarkable advantages, RF-SETs have been substituted to SETs in many measurement setups. For example, RF-SETs have been implemented as a single-electron electrometer [5], and more widely, as a detector for charge qubits [6], [7], single-electron dynamics [8], millimeter-wave single photons [9], and quantum dynamics of nanomechanical resonators [10].

The response of the RF-SET depends on a number of design parameters such as the amplitude and frequency of the modulating and carrier signals, the SET resistance, the resonant-circuit Q-factor, the operating temperature, and the insertion losses present in the conductance path between the tank circuit and the cryogenic amplifier [11]. Although the sensitivity of the RF-SET is expected to reach the shot-noise limit, the theoretical limit is still approximately five times higher than the best reported experimental charge sensitivity [4]. In order to realize the theoretical limit of the charge sensitivity, it is imperative to understand how the different parameters of the measurement system affect the performance of the real-time measurement setup. As quite a few parameters are prefixed and cannot be changed easily, the simulation of an entire system is crucial. However, the simulation of the RF-SETs is quite challenging because it has to deal with both the single-electron tunneling model for the SETs and the high-frequency components such as directional couplers and coaxial cables. For the design considerations of the *LC*-resonant circuit and analysis of the RF-SET response and sensitivity, the numerical analysis was reported in [12]. Until now, to the best of our knowledge, no detailed simulation of the whole RF-SET measurement system has been reported. Moreover, the real-time whole measurement setup is very difficult to implement in the numerical simulation. Therefore, the aim of this paper is to present the design and analysis method for the RF-SETs by adopting a suitable SET model that incorporates various physical effects, including the background charge, the temperature effects, and the other components of the RF-SET.

In the present paper, the SET characteristics were modeled using the analytical SET model [13], which was incorporated into a circuit simulator using the analog hardware description language (AHDL) [14]. The analytical SET model was developed within the scope of the "orthodox theory" of the single-electron tunneling [19], [20]. The advantage of this modeling is that the SET model is implemented as a separate module in the SPICE circuit simulator, rather than rigorously solving the SET characteristic equations, along with other nonlinear components of the RF-SET. Moreover, the analytical model enables a faster circuit analysis [15] compared to the Monte Carlo

Manuscript received April 13, 2007. The review of this paper was arranged by Associate Editor E. Wang.

M. Manoharan and B. Pruvost are with the Quantum Nanoelectronics Research Center and the Department of Physical Electronics, Tokyo Institute of Technology, Tokyo 152-8552, Japan (e-mail: mano@neo.pe.titech.ac.jp; benjamin@neo.pe.titech.ac.jp).

S. Oda is with the Quantum Nanoelectronics Research Center and the Department of Physical Electronics, Tokyo Institute of Technology, Tokyo 152-8552, Japan. He is also with the Solution Oriented Research for Science and Technology (SORST) Japan Science and Technology (JST), Saitama 332-0012, Japan (e-mail: soda@pe.titech.ac.jp).

H. Mizuta is with the School of Electronics and Computer Science, The University of Southampton, Southampton SO17 1BJ, U.K., the Department of Physical Electronics, Tokyo Institute of Technology, Tokyo 152-8552, Japan, and with the Solution Oriented Research for Science and Technology (SORST) Japan Science and Technology (JST) (e-mail: hm2@ecs.soton.ac.uk).

Digital Object Identifier 10.1109/TNANO.2007.915020

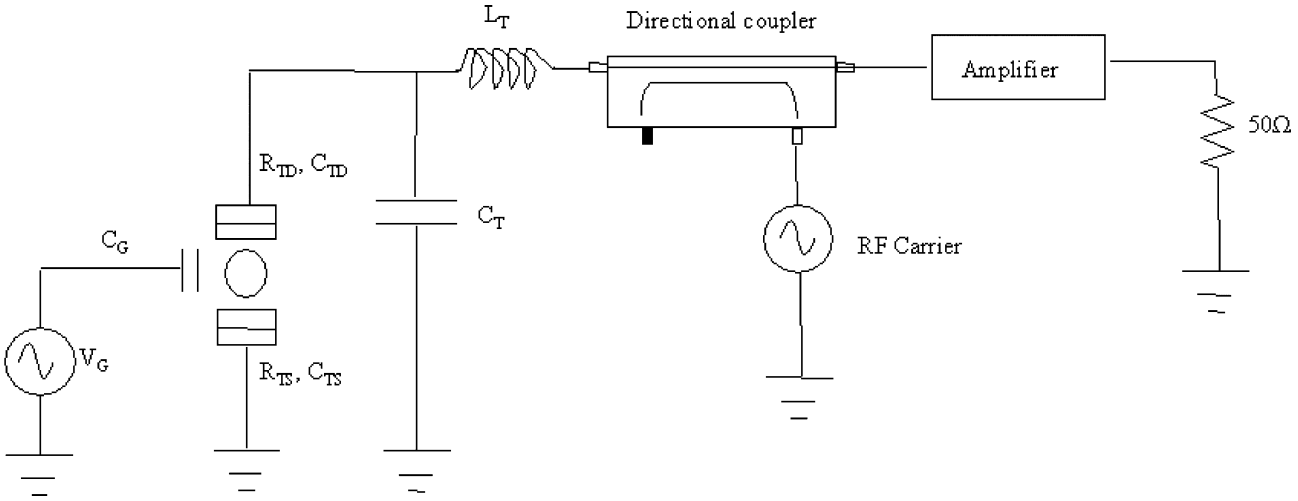

Fig. 1. Schematic diagram of the simulated reflection RF-SET measurement setup.

simulations (for example, SIMON [16] and KOSEC [17]). The SPICE equivalent models were used to implement all the other components of the RF-SET measurement system. Even though the reflection-type RF-SETs are discussed in this paper, the developed hybrid simulation method can also be equally used to analyze the transmission-type RF-SETs and other RF reflection measurements like RF quantum point contacts (RF-QPCs) and RF scanning tunneling microscopes (RF-STMs).

In Section II, the analytical modeling of the SET and its characteristics validation with the widely used Monte Carlo simulator are discussed. Meanwhile, the impact of key circuit parameters on the RF-SET response in terms of the SNR of the reflected signal is discussed in Section III.

II. Modeling and Evaluation of the SET and RF-SET

The schematic of the reflection RF-SET as implemented in our simulation is shown in Fig. 1. The SET consists of two tunnel junctions with capacitances C_{TD} and C_{TS} and resistances R_{TD} and R_{TS}. The SET is coupled via the gate capacitance C_G to the external input signal. The RF carrier is directed toward the SET through the coupled port of the directional coupler. The carrier frequency is chosen such that it is in resonance with the tank circuit formed by the combination of inductor L_T and capacitor C_T. The through port of the directional coupler guides the reflected signal from the SET to the amplifier.

A. SET Analytical Model

The simulation of the SET along with other components of the RF-SET in the SPICE environment is fairly difficult because of the electrical characteristics of the SET that result from the Coulomb blockade and oscillation phenomenon. A compact and physically based SET analytical model was used to simulate the SET characteristics [13]. A similar kind of analytical model was already shown to be accurate for the SET logic circuit simulation in both static and dynamic regimes [18]. Contrary to other reported analytical models [15], this model is based on the "orthodox" theory of single-charge tunneling and master equation method [19], [20], the methods that show no voltage limitation in the scope of this theory. The analytical model is based on the following assumptions: 1) inside the island, the electron energy spectrum is continuous, i.e., any quantization of electronic energy is ignored; 2) the time taken by the electron tunneling through the barrier is assumed to be negligibly small in comparison with other time scales; and 3) coherent quantum processes consisting of several simultaneous tunneling events ("cotunneling") are ignored. Using a capacitor connected to the island with a specific charge can include a background charge effect on the SET characteristics. This model is verified against the simulated data from the Monte Carlo simulator CAMSET [21]. This Monte Carlo simulator has already been used to verify the newly developed analytical model [22]. Fig. 2 shows the accuracy of our model for the different values of drain-to-source voltages. Several drain currents (I_{DS}) obtained at different temperature levels (from 50 to 300 K) with $V_{GS} = 0$ V and without a background charge are shown in Fig. 3. It can be noted that our model is in

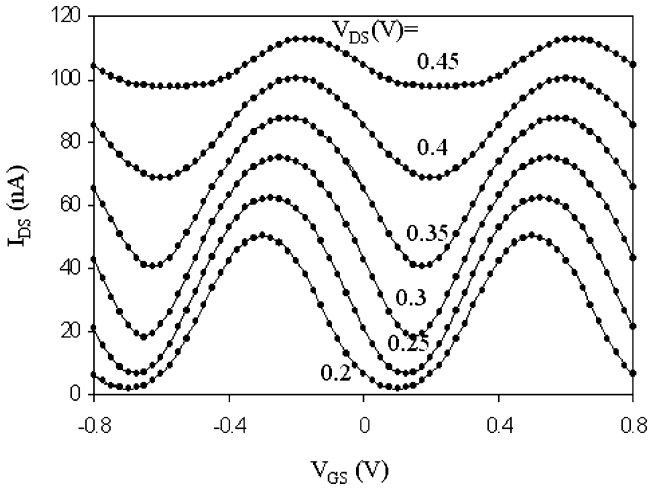

Fig. 2. I_{DS}–V_{GS} verification of the SET for a symmetric device with $C_G = 0.2$ aF, $C_{TD} = C_{TS} = 0.15$ aF, and $R_{TD} = R_{TS} = 1$ MΩ, at $T = 173$ K. Dotted lines represent the Monte Carlo simulation (CAMSET) [21] and solid lines represent the analytical model simulation.

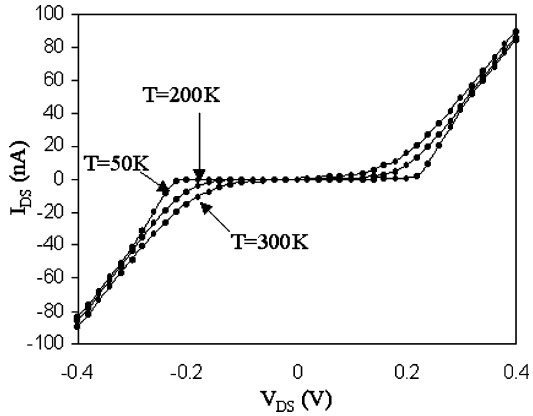

Fig. 3. I_{DS}–V_{DS} verification of the analytical model at different temperature levels for a symmetric device with $C_G = 0.2$ aF, $C_{TD} = C_{TS} = 0.15$ aF, and $R_{TD} = R_{TS} = 1$ MΩ. Dotted lines represent the Monte Carlo simulation (CAMSET) [21] and solid lines represent the analytical model simulation.

perfect accordance with the CAMSET simulation. This model has been validated until $T < e^2/(10\ k_B C_{\rm island})$, where k_B is the Boltzmann constant and $C_{\rm island}$ is the total island capacitance with respect to the ground.

B. Radio Frequency Components Model

SPICE is a powerful tool that can be used even for RFs by employing the proper models for each component at the frequencies of interest. In the RF-SET measurement setup, RF components, directional coupler, coaxial cable, and RF amplifier are used. The directional coupler was implemented using the equivalent circuit consisting of two transformers cross-coupled at the input port [23]. The coupling and directivity of the coupler can be varied by a proper choice of the primary and secondary inductances of the transformers. Insertion loss and frequency-dependent characteristics of the coupler can also be introduced in this model by including a resistor and a capacitor along with the primary and the secondary inductors. A directional coupler with 20 dB coupling was used in the simulation results. It should be noted that SPICE has models for lossy coaxial transmission lines with dielectric and conductor losses.

C. Linear Analysis of the RF-SET

At a higher frequency, the most crucial requirement is proper matching in the circuit; otherwise, the signal will be lost through reflection and radiation. In the RF-SET, the *LC*-resonant circuit effectively couples the 50 Ω higher frequency measurement part to the high resistance SET. For the small signal circuit analysis, we substitute the SET with an effective differential resistance R_d. The input impedance at the inductor L_T looking into the SET is given by

$$Z_{\rm Tot} = i\varpi L_T + \frac{1}{i\varpi C_T + R_d^{-1}} \tag{1}$$

where C_T is the tank circuit capacitance.

By performing a linear circuit analysis, the input impedance at the resonant frequency can be simplified to

$$Z_{\rm Tot} = \frac{L_T}{C_T R_d}. \tag{2}$$

The voltage reflection coefficient (at the inductor, which is the amplitude of the reflected voltage wave normalized to the amplitude of the incident voltage wave, is given by

$$\Gamma = \frac{Z_{\rm Tot} - R_0}{Z_{\rm Tot} + R_0} \tag{3}$$

where R_0 is the characteristic impedance of the coaxial cable (typically 50 Ω). For $Z_{\rm Tot} = 50\,\Omega$, the SET is perfectly matched with the RF part of the circuit, but the value of $Z_{\rm Tot}$ varies according to the electrodynamic condition of the SET.

The characteristic impedance R_0 of the high-frequency measurement setup and the SET differential resistance R_d influence the quality factor of the tank circuit. To analyze the matching condition qualitatively, the *LC* resonator can be considered separately from the SET and the remaining part of the measurement setup. Considering the tank circuit along with the characteristics impedance of the coaxial cable alone, the unloaded quality factor Q can be written as

$$Q = \frac{\sqrt{L_T/C_T}}{R_0} \tag{4}$$

where R_0, L_T, and C_T are in a series combination, and can be analyzed by the series resonant circuit method.

If the impact of the SET differential resistance on the tank circuit quality factor is considered (R_d, L_T, and C_T form a parallel combination), then SET quality factor can be given by

$$Q_{\rm SET} = \frac{R_d}{\sqrt{L_T/C_T}}. \tag{5}$$

In practice, the individual quality factors will have the effect of lowering the overall or loaded quality factor [24]. Thus, the loaded quality factor is

$$\frac{1}{Q_L} = \frac{1}{Q} + \frac{1}{Q_{\rm SET}}. \tag{6}$$

SET quality factor $Q_{\rm SET}$ is decided by the SET conductance and cannot be used as a tunable parameter. The unloaded quality factor Q can be varied by tuning the tank circuit inductor and capacitor values. The unloaded quality factor is used as a variable to analyze the response of the RF-SET in this simulation.

At resonant frequency, the reflection coefficient can be simplified to

$$\Gamma = -1 + \frac{2}{1 + Q^2(R_0/R_d)} Q^2 \frac{R_0}{R_d} \tag{7}$$

by substituting (1) in (3). Hence, for the value of $Q^2 = R_d/R_0$, a perfect matching is achieved. However, the differential resistance R_d is decided by the operating condition of the SET.

III. Impact of Key Circuit Parameters on RF-SET Response

The dependence of the RF-SET response was analyzed as a function of the RF carrier power and the temperature, the tunnel junction resistances R_{TD} and R_{TS} (symmetric tunnel junction resistances and capacitances were assumed throughout the simulation), the tank circuit unloaded quality factor (Q), the second and third overtones of the incident signal resonant with the tank circuit, the insertion loss present in the conducting path between the SET and the cryogenic amplifier, and the tank circuit inductor parasitics. In these simulation results, a 2 MHz gate signal with an amplitude of 0.1 $\mathrm{mV_{p\text{-}p}}$ was used. Tunnel junction capacitances of 1 aF and a gate capacitance of 2 aF were used. The value of the reflected signal SNR was used to compare the response for the various parameters in pure RF mode excitation [25]. The RF-SET response was studied by performing the transient response analysis. In addition, the Fourier transform was done to evaluate the SNR of the reflected signal. The amplifier model used in this simulation was ideal, so it is noise-free. Losses associated with the directional coupler and the inductor (in the chip inductor model) set the noise floor in this simulation. The analytical SET noise modeling and the RF-SET noise analysis will be the bases of our future works. In our simulation, the analytical model was used within the limitation of a carrier frequency much less than I/e, which ensures that the quasi-stationary state is reached throughout the period of oscillations [26]. In experiments, the interconnect capacitance associated with the gate, source, and drain terminals is much larger than the device capacitances. Thus, the total island capacitance to the ground is given by $C_{\mathrm{island}} = C_{TD} + C_{TS} + C_G$. This condition assures that the SET characteristics are not affected by the capacitances of the neighboring devices [15].

A. Dependence on RF Carrier Power and Temperature

The RF-SET response depends on the amplitude of the RF signal at the SET, which has to be less than e/C_Σ for a symmetric SET. Fig. 4(a) shows the RF-SET response as a function of RF carrier power at the source for $T = 300$ mK, $R_{\mathrm{SET}} = 52\ \mathrm{k\Omega}$ ($R_{\mathrm{SET}} = R_{TD} + R_{TS}$), and $Q = 45$. The RF-SET response is high for the specific carrier power and is degraded for other values. To realize a maximum response, the RF amplitude has to be chosen within the Coulomb blockade threshold voltage. The RF-SET response degrades if the carrier power at the SET is too small due to the thermal noise contribution from other components. The RF-SET response simulation results as a function of temperature are shown in Fig. 4(b) for $R_{\mathrm{SET}} = 100\ \mathrm{k\Omega}$ and -71 dBm carrier power at the source. From the simulated response, it can be understood that the RF-SET response increases as the temperature decreases and saturates below 1.5 K. This is due to the increase of the peak-to-valley ratio of the Coulomb blockade SET current [27]. A higher peak-to-valley ratio of the SET current greatly modulates the SET resistance so that the RF-SET response increases as the temperature decreases. For the purpose of comparing simulation results, all of the following simulations were performed at a constant temperature $T = 300$ mK.

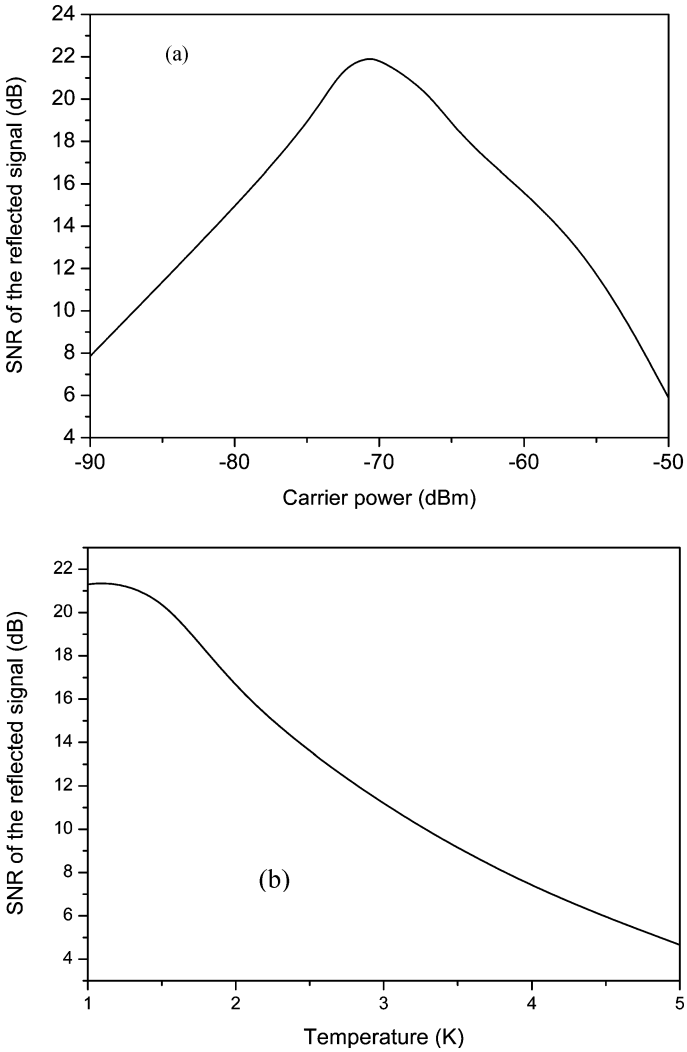

Fig. 4. SNR of the reflected signal. (a) As a function of carrier power at the source for $T = 300$ mK. (b) As a function of temperature for the carrier power of –71 dBm at source.

B. SET Resistance Dependence

To estimate the dependence of the RF-SET response on tunnel junction resistances, the latter were varied from 26 to 150 kΩ by keeping other parameters constant at 300 mK. As the cotunneling was not taken into account, we did not perform any simulation for tunnel junction resistances lower than 26 kΩ because of the inaccuracy of the orthodox theory in this range of values. Fig. 5 shows the SNR of the reflected signal as a function of tunnel junction resistance variation for various values of Q-factors at resonant frequency. The RF-SET response is degraded linearly with the increase in tunnel junction resistance. It can be noticed that the response improves with the increase in Q-factor for the small values of Q, whereas an increase in Q-factor degrades the response. As per (7), for the values of $R_d = 100\ \mathrm{k\Omega}$ and $Q = 45$, the reflection coefficient attains its minimum value. However, the response tends to improve further with the decrease in R_{SET} value. This is due to the decrease of the resistance mismatch between the RF part characteristics resistance R_0 and the SET, which is important for the signal

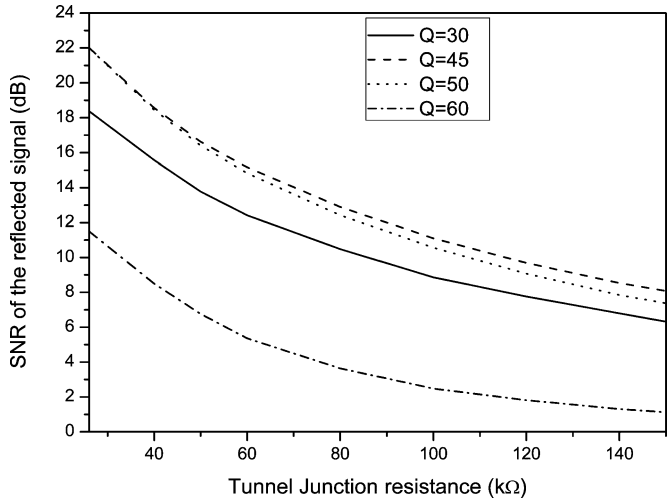

Fig. 5. Reflected signal SNR as a function of tunnel junction resistance for various unloaded quality factors Q. $T = 300$ mK and $f = f_0$.

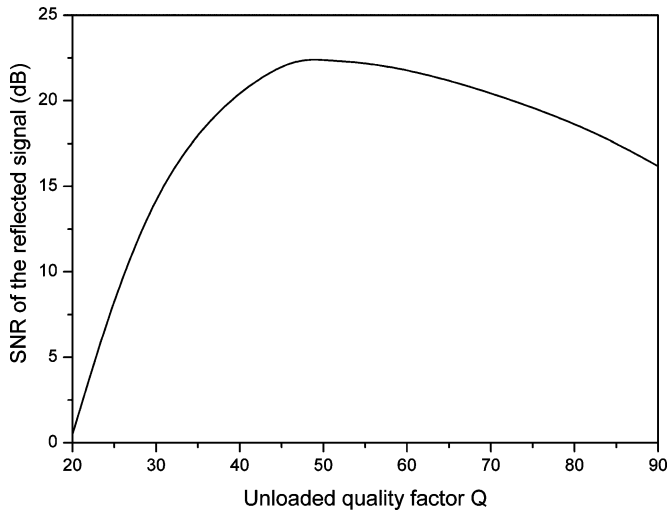

Fig. 6. RF-SET response as a function of unloaded quality factor Q. $T = 300$ mK and $R_{\rm SET} = 100\,\text{k}\Omega$.

propagation at higher frequencies. This simulation result indicates the importance of low tunnel junction resistance SET in realizing a high charge sensitivity RF-SET.

C. Quality Factor Dependence

The SET quality factor $Q_{\rm SET}$ depends on the operating condition of the SET; hence, it cannot be used as an RF-SET design parameter. However, the unloaded quality factor Q can be tuned by varying the tank circuit inductor and capacitor values. The unloaded Q-factor dependence of the RF-SET response at resonant frequency is shown in Fig. 6 for $T = 300$ mK and $R_{\rm SET} = 100\,\text{k}\Omega$. It shows that the response initially increases with the increase in Q-factor for small values and reaches its maximum at $Q = 45\ (=\sqrt{R_d/R_0})$, as predicted by the matching condition given by (7). For this value of the Q-factor, the reflection coefficient attains its minimum value in the RF-mode excitation. Nonetheless, a further increase in the Q-factor introduces a mismatch in the reflection path and degrades the response.

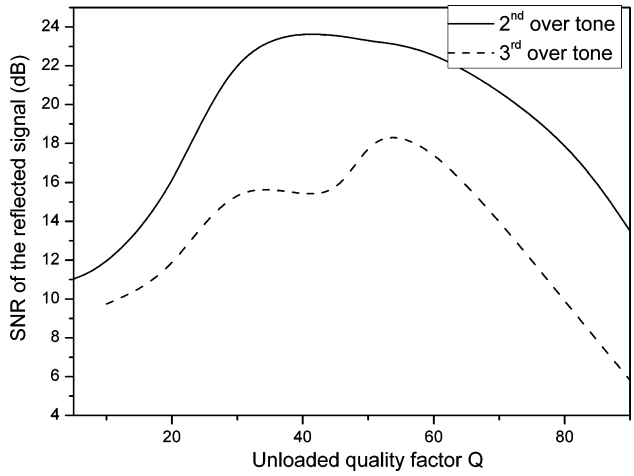

Fig. 7. SNR of the reflected signal for the second and third overtones of the carrier wave resonance with the tank circuit for various unloaded quality factor Q. $T = 300$ mK and $R_{\rm SET} = 100\,\text{k}\Omega$.

D. Resonant Overtone Analysis

Nonlinear controllability of the SET current by the gate charge is used to realize the RF-mixing [28]. The significant I–V nonlinearity can be used to monitor the overtones of the reflected signal from the RF-SET. Turin and Korotkov [29] proposed this overtone operation mode. The advantages of monitoring the overtones are in the form of separate frequencies for the transmitted carrier and the modulated reflected signal (which may be preferred in experiments), and the absence of a high-amplitude reflected power when the SET is in a Coulomb blockade state. The problem associated with the overtone monitoring is the requirement of an amplitude incident signal larger than the incident signal monitoring. Fig. 7 shows the response for the second overtone $f = f_o/2$ (where f_o is the resonant frequency of the tank circuit and f is the exciting carrier frequency), and for the third overtone $f = f_o/3$ of the incident signal with the tank circuit for $T = 300$ mK and $R_{\rm SET} = 100\,\text{k}\Omega$. As seen in Fig. 7, the second and third resonant overtones responses are reasonably good due to the substantial nonlinearity of the SET I–V characteristics. By comparing Figs. 6 and 7, it can be concluded that the response of the second and third overtones and regular $f = f_o$ mode are comparable. The potential of the overtone usage can thus be exploited in the experimental setup.

E. Dependence on Insertion Loss Between the Tank Circuit and the Cryogenic Amplifier

Because the amplitude of the reflected signal from the SET is very small, it will be easily affected by the noise present in the path between the tank circuit and the cryogenic amplifier. To reduce the coaxial cable noise, a superconducting niobium cable is used in the conduction path between the tank circuit and the cryogenic amplifier [25]. However, the connectors' mismatch loss and insertion losses of the bias Tee and directional coupler (which can be collectively called "feed-through loss") cannot be reduced to 0 dB by using the currently available state-of-the-art performance components. Therefore, it is necessary to analyze the response degradation with the increase

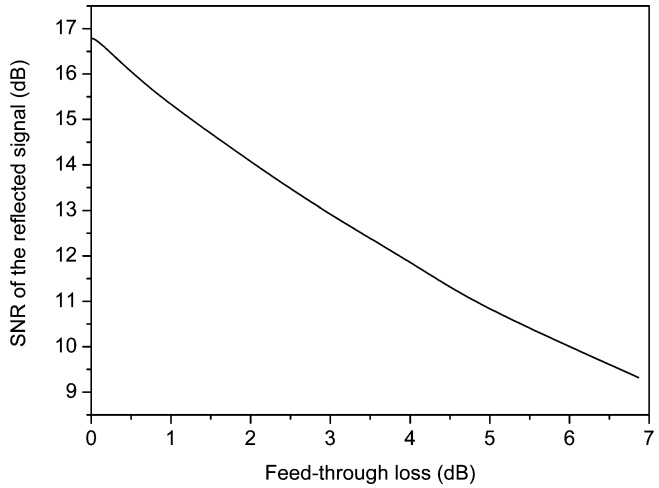

Fig. 8. SNR of the reflected signal as a function of feed-through loss between the tank circuit and the cryogenic amplifier. $T = 300$ mK, $Q = 45$, and $R_{\rm SET} = 100$ kΩ.

in insertion loss. Fig. 8 shows the RF-SET response dependency on the feed-through loss at resonant frequency for $T = 300$ mK and $R_{\rm SET} = 100$ kΩ. The feed-through loss was realized in the simulation by using the lossy uncoupled transmission line model [14]. In order to include the insertion losses of the bias Tee and directional coupler, more noise was introduced by using the lossy transmission line model. It can be understood from the simulation result that the response degrades linearly with the increase in insertion loss. In experimentally reaching the theoretical limitation of the charge sensitivity, this insertion loss, which cannot be reduced beyond a certain value, becomes a problem. Even though the cryogenic amplifier noise temperature was very low in the recently reported experimental work of [4], the effect of feed-through loss on RF-SET performance has already been reported.

F. Effect of Inductor Parasitics

For the *LC*-resonant circuit, a chip inductor or normal conductor on-chip spiral inductor is used. Due to the spreading resistance and eddy current losses associated with the inductor, parasitic resistances and capacitances also exist along with the ideal inductor. These parasitics affect the RF-SET response by introducing an impedance mismatch in the conductance path and detuning the resonant frequency of the tank circuit. The lumped element equivalent circuit of a typical chip inductor as given by the manufacturer is shown in Fig. 9, where R_1, R_2, $R_{\rm var}$, and C_1 are parasitics resistances and capacitance, respectively [30]. This lumped element equivalent circuit was used to simulate the effect of inductor parasitics on the RF-SET response. Table I shows a comparison of the simulation results between the ideal inductor and the chip inductor. It clearly indicates that the parasitics considerably degrade the response. Also, for this lumped element values, it was found that the resistance R_2 degrades the response greatly compared to other resistances. In order to get a maximum RF-SET response, parasitic resistances have to be reduced, which may be achieved by fabricating the on-chip inductor with a superconductor.

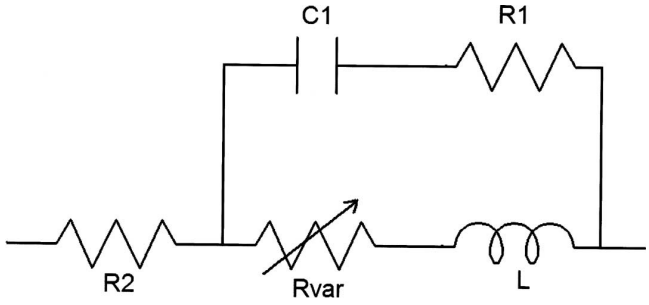

Fig. 9. Real-time lumped element equivalent circuit of the chip inductor [29]. $R_1 = 37\ \Omega, R_2 = 1.4\ \Omega, R_{\rm var} = k \times \sqrt{f}\ \Omega, k = 5.74 \times 10^{-4}, C_1 = 0.143$ pF, $L = 615$ nH, where f is the operating frequency.

TABLE I
COMPARISON OF THE RF-SET RESPONSE FOR THE IDEAL INDUCTOR AND THE LUMPED ELEMENT EQUIVALENT CIRCUIT OF THE CHIP INDUCTOR MODEL

Q factor	Response for the ideal inductor model (dB)	Response for the chip Inductor model (dB)
45	22.56	14.83
50	22.37	13.69
60	22.07	15.07

IV. CONCLUSION

A physically based analytical SET model combined with a SPICE equivalent circuits simulation was adopted to analyze the real-time RF-SET measurement setup. The impact of the feed-through loss present between the tank circuit and the cryogenic amplifier and inductor parasitics, along with the other key circuit parameters, were analyzed. It was demonstrated that even though the cryogenic amplifier noise temperature is reduced in the present RF-SET measurement setups, the charge sensitivity could not be improved greatly unless the effects of the feed-through loss are taken into consideration properly. Finally, the impact of impedance mismatch and insertion loss associated with the parasitics resistances and capacitances of the inductor on the RF-SET response were shown by using a real-time lumped element equivalent circuit analysis.

REFERENCES

[1] M. H. Devoret and R. J. Schoelkopf, "Amplifying quantum signals with the single-electron transistor," *Nature*, vol. 406, pp. 1039–1046, Aug. 2000.

[2] R. J. Schoelkopf, P. Wahlgren, A. A. Kozhevnikov, P. Delsing, and D. E. Prober, "The radio-frequency single-electron transistor (RF-SET): A fast and ultrasensitive electrometer," *Science*, vol. 280, pp. 1238–1242, May 1998.

[3] T. Fujisawa and Y. Hirayama, "Charge noise analysis of an AlGaAs/GaAs quantum dot using transmission-type radio-frequency single-electron transistor technique," *Appl. Phys. Lett.*, vol. 77, pp. 543–545, Jul. 2000.

[4] H. Brenning, S. Kafanov, T. Duty, S. Kubatkin, and P. Delsing, "An ultrasensitive radio-frequency single-electron transistor working up to 4.2 K," *J. Appl. Phys.*, vol. 100, pp. 114321-1–114321-6, Dec. 2006.

[5] J. Bylander, T. Duty, and P. Delsing, "Current measurement by real-time counting of single electrons," *Nature*, vol. 434, pp. 361–364, Mar. 2005.

[6] Y. Makhlin, G. Schön, and A. Shnirman, "Quantum-state engineering with Josephson-junction devices," *Rev. Mod. Phys*., vol. 73, pp. 357–400, Apr. 2001.
[7] A. Aassime, G. Johansson, G. Wendin, R. J. Schoelkopf, and P. Delsing, "Radio-frequency single-electron transistor as readout device for qubits: Charge sensitivity and backaction," *Phys. Rev. Lett*., vol. 86, pp. 3376–3379, Apr. 2001.
[8] W. Lu, Z. Ji, L. Pfeiffer, K. W. West, and A. J. Rimberg, "Real-time detection of electron tunnelling in a quantum dot," *Nature*, vol. 423, pp. 422–425, May 2003.
[9] T. R. Stevenson, A. Aassime, P. Delsing, R. Schoelkopf, K. Segall, and C. M. Stahle, "RF single electron transistor readout amplifiers for superconducting astronomical detectors of X-ray to sub-mm wavelengths," *IEEE Trans. Appl. Supercond*, vol. 11, no. 1, pp. 692–695, Mar. 2001.
[10] M. D. LaHaye, O. Buu, B. Camarota, and K. C. Schwab, "Approaching the quantum limit of a nanomechanical resonator," *Science*, vol. 304, pp. 74–77, Apr. 2004.
[11] M. Manoharan, H. Mizuta, and S. Oda, "Hybrid simulation of the RF-SET and its charge sensitivity analysis," in *Proc. 2006 Int. Conf. Solid State Devices Mater., Extended Abstract*, pp. 736–737.
[12] V. O. Turin and A. N. Korotkov, "Numerical analysis of radio-frequency single-electron transistor operation," *Phys. Rev. B*, vol. 69, pp. 195310-1–195310-13, May 2004.
[13] B. Pruvost, H. Mizuta, and S. Oda, "3-dimensional design and analysis of functional NEMS-gate MOSFETs and SETs," *IEEE Trans. Nanotechnol*., vol. 6, no. 2, pp. 218–224, Mar. 2007.
[14] SmartSPICE. (2005). User's guide [Online]. Available: www.silvaco.com
[15] S. Mahapatra, V. Vaish, C. Wasshuber, K. Banerjee, and A. M. Ionescu, "Analytical modeling of single electron transistor for hybrid CMOS-SET analog IC design," *IEEE Trans. Electron Devices*, vol. 51, no. 11, pp. 1772–1782, Nov. 2004.
[16] C. Wasshuber, *Computational Electronics*. New York: Springer-Verlag, 2002.
[17] Y. S. Yu, J. H. Oh, S. W. Hwang, and D. Ahn, "Implementation of single electron circuit simulation by SPICE: KOSECSPICE," in *Proc. Asia Pac. Workshop Fundam. Appl. Adv. Semicond. Device*, 2000, pp. 85–90.
[18] S. Mahapatra, A. M. Ionescu, and K. Banerjee, "A quasianalytical SET model for few electron circuit simulation," *IEEE Electron Device Lett*., vol. 23, pp. 366–368, Jun. 2002.
[19] K. K. Likharev, "Single-electron devices and their applications," *Proc. IEEE*, vol. 87, no. 4, pp. 606–632, Apr. 1999.
[20] S. Mahapatra, V. Pott, S. Ecoffey, A. Schmid, C. Wasshuber, J. W. Tringe, Y. Leblebici, M. J. Declercq, K. Banerjee, and A. M. Ionescu, "SETMOS: A novel true hybrid SET-CMOS high current Coulomb blockade oscillation cell for future nano-scale analog ICs," in *Proc. IEDM*, 2003, pp. 703–706.
[21] M. Kirihara, K. Nakazato, and M. Wagner, "Hybrid circuit simulator including a model for single electron tunneling devices," *Jpn. J. Appl. Phys*., vol. 38, pp. 2028–2032, 1999.
[22] K. Uchida, K. Matsuzawa, J. Koga, R. Ohba, S. Takagi, and A. Toriumi, "Analytical single-electron transistor (SET) model for design and analysis of realistic SET circuits," *Jpn. J. Appl. Phys. B*, vol. 39, no. 4, pp. 2321–2324, 2000.
[23] S. Hamilton, *An Analog Electronics Companion: Basic Circuit Design for Engineers and Scientists*. Cambridge, U.K.: Cambridge Univ. Press, 2003, ch. 5.12.
[24] D. M. Pozar, *Microwave Engineering*. Hoboken, NJ: Wiley, 2005, ch. 6.
[25] A. Aassimee, D. Gunnarsson, K. Bladh, P. Delsing, and R. J. Schoelkopf, "Radio-frequency single-electron transistor: Toward the shot-noise limit," *Appl. Phys. Lett*., vol. 79, no. 24, pp. 4031–4033, 2001.
[26] A. N. Korotkov and M. A. Paalanen, "Charge sensitivity of radio frequency single-electron transistor," *Appl. Phys. Lett*., vol. 74, pp. 4052–4054, 1999.
[27] L. P. Kouwenhoven, C. M. Markus, P. L. McEuen, S. Tarucha, R. M. Westervelt, and N. S. Wingreen, "Electron transport in quantum dots," in *Mesoscopic Electron Transfer,* L. Sohn, L. P. Kouwenhoven, and G. Schön, Eds. Dordrecht, The Netherlands: Kluwer, 1997, pp. 105–215.
[28] R. Knobel, C. S. Yung, and A. N. Cleland, "Single-electron transistor as a radio-frequency mixer," *Appl. Phys. Lett*., vol. 81, pp. 532–534, Jul. 2002.
[29] V. O. Turin and A. N. Korotkov, "Analysis of the radio-frequency single-electron transistor with large quality factor," *Appl. Phys. Lett*., vol. 83, pp. 2898–2900, Oct. 2003.
[30] SPICE models for coilcraft RF inductor. (2005). [Online]. Available: www.coilcraft.com

M. Manoharan was born in Coimbatore, India. He received the B.E. degree in electronics and communication from Bharathiar University, Coimbatore, in 2000, and the M.Tech. degree in electrical engineering (specializing in microwave engineering) from the Indian Institute of Technology (IIT), Kanpur, India, in 2005. He is currently working toward the Ph.D. degree at the Physical Electronics Department, Tokyo Institute of Technology, Tokyo, Japan.

His current research interests include the silicon nanoelectronics, its fabrication techniques, and quantum effect simulation.

Benjamin Pruvost received both the Dipl.Ing. degree from the Ecole Supérieure d'Electricité (Supélec), Gif-sur-Yvette, France, and the M.S. degree in physical electronics in 2006 from Tokyo Institute of Technology, Tokyo, Japan, where he is currently working toward the Ph.D. degree at the Quantum Nanoelectronics Research Center.

His current research interests include the modeling and design of new hybrid nanodevices.

Hiroshi Mizuta (M'89) received the B.S. and M.S. degrees in physics and the Ph.D. degree in electrical engineering from Osaka University, Osaka, Japan, in 1983, 1985, and 1993, respectively.

In 1985, he joined the Central Research Laboratory, Hitachi Ltd., Tokyo, Japan, where he has been engaged in research on high-speed heterojunction devices and resonant tunneling devices. From 1989 to 1991, he worked on quantum transport simulation. From 1997 to 2003, he worked on single-electron devices and other quantum devices as the Laboratory Manager and Senior Researcher at the Hitachi Cambridge Laboratory, U.K. From 2003 to 2007, he was an Associate Professor of physical electronics at the Tokyo Institute of Technology, Tokyo. Since April 2007, he has been a Professor of nanoelectronics at the University of Southampton, Southampton, U.K. He is also with the Solution Oriented Research for Science and Technology (SORST) Japan Science and Technology (JST), Saitama, Japan. His current research interests include silicon-based nanoelectronics, silicon nanostructures such as silicon nanodots and nanowires, silicon nanoelectromechanical devices for information processing, and *ab initio* calculations of nanomaterial properties, and quantum transport in silicon nanostructures. He is the author or coauthor of more than 200 scientific papers and several books including *Physics and Applications of Resonant Tunnelling Diodes* (Cambridge University Press). He holds more than 50 patents.

Dr. Mizuta is a member of the Physical Society of Japan, the Japan Society of Applied Physics, the Institute of Physics, and the Electron Device Society of the IEEE.

Shunri Oda (M'89) received the B.Sc. degree in physics and the M.S. and Ph.D. degrees in physical information processing from Tokyo Institute of Technology, Tokyo, Japan, in 1974, 1976, and 1979, respectively.

He is currently a Professor in the Department of Physical Electronics and Quantum Nanoelectronics Research Center, Tokyo Institute of Technology. He is also with the Solution Oriented Research for Science and Technology (SORST) Japan Science and Technology (JST), Saitama, Japan. His current research interests include the fabrication of silicon quantum dots by pulsed plasma processes, single-electron tunneling devices based on nanocrystalline silicon, ballistic transport in silicon nanodevices, silicon-based photonic devices, and high-K gate oxide ultrathin films prepared by atomic layer metalorganic chemical vapor deposition (MOCVD). He is the author or coauthor of more than 200 papers published in journals and conference proceedings.

Dr. Oda is a member of the Electrochemical Society, the Materials Research Society, and the Japan Society for Applied Physics. He is also a Distinguished Lecturer of the IEEE Electron Devices Society.